Stem Cell Research & Therapy

RESEARCH

Open Access

Device encapsulated MSCs for adaptive secretome therapy to effectively target ischaemic heart injury

Andrew R. Kompa[1,2†], David W. Greening[3,4,5†], Jarmon G. Lees[1,2,6†], Anne M. Kong[1,2], Jonathon Cross[3], Ashley Nowland[1], Ren J. Phang[1], Saba Naghipour[1], Yali Deng[1,2], Jack R. T. Darby[7], Lina Mariana[1], Cameron Kos[1], Tanya Hall[8], Andrew Newcomb[2,9], James J. H. Chong[10,11], Rebecca H. Ritchie[3,5,6], Janna L. Morrison[7,12], Klearchos K. Papas[13,14], Kilian Kelly[15], Derek J. Hausenloy[16,17,18,19], Thomas Loudovaris[1,14] and Shiang Y. Lim[1,2,6,19,20*]

Abstract

Background Effective long-term strategies to protect the ischaemic heart remain a significant challenge. Mesenchymal stromal cells (MSCs) offer therapeutic potential primarily through their secretome, a bioactive factor-rich milieu with broad beneficial effects. However, existing delivery methods have not demonstrated sustained cardioprotection. The objective of this study was to evaluate a clinically translatable approach for sustained MSC-secretome delivery to achieve long-term cardioprotection.

Methods Cymerus MSCs, derived from human induced pluripotent stem cells (iPSCs), were encapsulated in a Procyon immunoisolation device and implanted subcutaneously in adult Sprague Dawley rats with chronic myocardial ischaemia-reperfusion injury. A human iPSC-derived engineered cardiac microtissue model was used to simulate ischaemia-reperfusion injury and assess cardioprotective effects in a human context. Proteomic analysis was performed to characterize adaptive changes in MSCs and their secretome post-implantation.

Results The MSC-loaded Procyon device significantly improved cardiac function and reduced adverse left ventricular remodelling over 12 weeks in both young and middle-aged, male and female rats. The encapsulated MSCs remained viable and retained the ability to release therapeutic secretome at 12 weeks post-implantation. In vitro, the MSC secretome protected human engineered cardiac microtissues from simulated ischaemia-reperfusion injury by restoring contractile function, improving cell viability, and reducing oxidative stress. Proteomic profiling of encapsulated MSC identified 179 unique cellular proteins post-implantation, associated with adaptive immune and inflammatory responses as well as wound healing. MSC secretome profiling revealed increased protein diversity associated with tissue repair and immune regulation, suggesting MSCs undergo an adaptive response to ischaemic conditions.

†Andrew R. Kompa, David W. Greening and Jarmon G. Lees have contributed equally to the study.

*Correspondence:
Shiang Y. Lim
mlim@svi.edu.au

Full list of author information is available at the end of the article

© The Author(s) 2025. **Open Access** This article is licensed under a Creative Commons Attribution-NonCommercial-NoDerivatives 4.0 International License, which permits any non-commercial use, sharing, distribution and reproduction in any medium or format, as long as you give appropriate credit to the original author(s) and the source, provide a link to the Creative Commons licence, and indicate if you modified the licensed material. You do not have permission under this licence to share adapted material derived from this article or parts of it. The images or other third party material in this article are included in the article's Creative Commons licence, unless indicated otherwise in a credit line to the material. If material is not included in the article's Creative Commons licence and your intended use is not permitted by statutory regulation or exceeds the permitted use, you will need to obtain permission directly from the copyright holder. To view a copy of this licence, visit http://creativecommons.org/licenses/by-nc-nd/4.0/.

Conclusion This translational study highlights a clinically viable, minimally invasive method for sustained cardioprotection, harnessing the MSC secretome to address a pivotal gap in current treatments for ischaemic heart disease.

Keywords Ischaemia-reperfusion injury, Myocardial ischaemia-reperfusion injury, Mesenchymal stromal cells, Immunoisolation device, Engineered cardiac microtissue, Induced pluripotent stem cells, Secretome

Introduction

Ischaemic heart disease remains the leading cause of death globally, with acute myocardial infarction (AMI) as a key clinical manifestation [1]. A major complication following AMI is adverse left ventricular remodelling, which often progresses to heart failure. Although several therapies are available to protect and repair the heart post-AMI, their effectiveness diminishes as the disease advances and the extent of damage increases [2]. Consequently, there is a critical unmet need for more effective long-term cardioprotective interventions. Stem cell therapy presents a promising opportunity to address this critical unmet need.

Mesenchymal stromal cells (MSCs), including those derived from human induced pluripotent stem cells (iPSCs), have shown promising potential to enhance cardiac function and structure, primarily through the paracrine activity of their secretome [3–5]. This secretome significantly improves the myocardial microenvironment by activating endogenous repair mechanisms; these include enhancing cell survival, promoting angiogenesis, resolving inflammation, and mitigating adverse remodelling [6, 7]. These promising preclinical findings on the MSC secretome are further reinforced by the ongoing first-in-human Phase 1 clinical trial, SECRET-HF, which specifically evaluates the cardioprotective effect of an extracellular vesicle-enriched secretome derived from cardiovascular progenitor cells generated from human iPSCs. While the trial is still underway, a case study of a patient with non-ischaemic dilated cardiomyopathy who received three intravenous infusions of secretome at three-week intervals showed promising cardiac improvements with no signs of immunogenicity [8].

Despite these advancements, clinical studies using MSCs from various sources have only demonstrated modest improvements in cardiac function. The limited success of MSC therapies is partly due to suboptimal cell delivery methods, which fail to fully harness the therapeutic potential of MSCs for sustained benefits and long-term cardiac repair [9, 10]. Current techniques, whether through intravenous, intracoronary, or direct intramyocardial delivery, often suffer from poor cell retention and high cell death rates in the harsh ischaemic environment, limiting the beneficial effects of the paracrine factors secreted by transplanted cells. These effects are typically short-lived, and the invasive nature of repeat administration poses a significant clinical challenge. While innovative approaches, such as cell encapsulating hydrogels, have shown promise in improving cell retention, they are still invasive and provide only temporary benefits due to their rapid biodegradation and death of the encapsulated MSCs within [9, 10].

In response to these challenges, we have pioneered an innovative and minimally invasive approach to harness MSCs as a living biodrug for the sustained release of their secretome, offering an effective strategy for long-term cardioprotection. Our method utilised a retrievable immunoisolation device implanted subcutaneously, ensuring both safety and controlled, long-term delivery of MSC-derived therapeutic secretome [11]. This device features a dual-membrane system: the inner membrane shields encapsulated cells from the host immune system while allowing the diffusion of nutrients and therapeutic outputs (including the secretome), and the outer membrane promotes blood vessel formation. In a preclinical study, subcutaneous implantation of these devices encapsulating human cardiac stem cells improved cardiac function and prevented maladaptive remodelling four weeks after non-reperfused MI in immunocompromised rats [11].

Despite these encouraging results, a significant gap remains in understanding the long-term efficacy of stem cell secretome therapies in immunocompetent models of chronic myocardial ischaemia-reperfusion injury. Addressing this limitation is essential for clinical translation, as immunocompromised models do not accurately reflect the immune responses seen in human patients, and short-term studies fail to capture the long-term remodelling that follows AMI. To bridge this translational gap, the present study evaluates the long-term effectiveness of MSC secretome-based therapies using clinical-grade MSCs derived from iPSCs in an immunocompetent rat model of chronic myocardial ischaemia-reperfusion injury, as well as in a human iPSC-derived cardiac microtissue model of ischaemia-reperfusion injury. The results show that sustained MSC secretome therapy provides long-term cardioprotection in age-appropriate models of chronic myocardial ischaemia-reperfusion injury in both sexes, as well as in preclinical human cardiac microtissues. Proteomic analysis further reveals that encapsulated MSCs exhibit an adaptive response by secreting a different combination of paracrine factors to target

and modulate cardiac pathologies, thereby enhancing cardioprotection.

Methods

Cell culture

Cymerus™ MSCs

Cymerus MSCs were generated from clinical-grade human induced pluripotent stem cells (iPSCs) as previously described [12] and supplied by Cynata Therapeutics Limited (Victoria, Australia). Upon receipt, the cryopreserved Cymerus MSCs (passage 2) were thawed, seeded on tissue culture flasks pre-coated with human fibronectin (1 mg/mL; Thermo Fisher Scientific, MA, USA) and human collagen I (3 µg/mL; Sigma-Aldrich, MO, USA), and expanded in serum-free expansion medium according to the manufacturer's instructions. Cymerus MSCs at passages 6–7 were used in the present study.

Human iPSC culture and differentiation

The human iPS-Foreskin-2 cell line, kindly provided by James A. Thomson (University of Wisconsin) [13] was maintained on vitronectin-coated plates in TeSR-E8 medium (STEMCELL Technologies, Vancouver, Canada) according to the manufacturer's protocol.

Engineered cardiac microtissue

Multicellular cardiac microtissues were generated by co-seeding iPSC-derived cardiomyocytes, endothelial cells, smooth muscle cells, and cardiac fibroblasts into ultra-low attachment round-bottom 96-well plates in spheroid induction medium, followed by centrifugation. After 48 h, the medium was replaced with cardiac spheroid maintenance medium. Compacted spheroids were then embedded in growth factor reduced Matrigel, transferred to anti-adherence-coated plates, and cultured under standard conditions on an orbital shaker for 3 days before experimental assays, allowing tissue maturation and establishment of baseline functionality.

Cell encapsulation

Procyon devices (Procyon Technologies LLC, AZ, USA) with 3 cm^2 single chamber were conditioned in 95% v/v ethanol for 10 min, 20% v/v ethanol for 10 min and rinsed in sterile phosphate buffered saline in sequential order. The conditioned Procyon devices were loaded with either human Cymerus MSCs (passage 6–7) suspended in 50 µL of Cymerus MSC serum-free expansion medium or 50 µL of Cymerus MSC serum-free expansion medium (as control) using a Hamilton syringe. The cell loading port was then sealed with medical grade adhesive silicone, type A (Nusil, CA, USA) and the excess port was trimmed off. The device was then placed in Cymerus MSC serum-free expansion medium at 37 °C in a humidified 5% CO_2 incubator for 1–3 days before implantation.

Animal ethics declaration

All experimental procedures were approved by the Animal Ethics Committee of St Vincent's Hospital and were conducted in accordance with the Australian National Health and Medical Research Council guidelines for the care and use of laboratory animals (AEC No. 011/22). All animal procedures conformed to the guidelines from Directive 2010/63/EU of the European Parliament on the protection of animals used for scientific purposes or the NIH guidelines. This study has been reported in accordance with the ARRIVE guidelines 2.0 to ensure transparent and comprehensive reporting of animal research.

Myocardial ischaemia-reperfusion injury (in vivo)

Part 1 dose-response study: Adult male Sprague Dawley rats aged 8–11 weeks were pretreated with antibiotics (enrofloxacin 175 mg/L, via drinking water) for 3 days prior to surgery. On day 0, anaesthetised animals (Alfaxan, 10 mL/kg, intravenous injection) were intubated and maintained on 2% isoflurane anaesthesia in oxygen at 70–75 breaths per minute. A left anterior thoracotomy was performed at the 4th intercostal space on the left-hand side and the left anterior descending coronary artery was ligated approximately 3 mm below the left atrium using a double knot 6 – 0 prolene monofilament polypropylene suture tied around a 20 mm length of PE100 tubing. Prior to occlusion, lignocaine (12 mg/kg, subcutaneous injection) was administered to reduce the incidence of arrhythmias. Successful coronary artery occlusion was indicated by visible blanching of the myocardium distal to the coronary ligation site and changes in electrocardiogram. Following 45 min occlusion, the PE tubing and suture were removed, and the thorax and muscle layers were closed with 4 – 0 silk sutures. The Procyon device containing either Cymerus MSCs (1×10^6, 2×10^6, 4×10^6 cells/device) or serum-free expansion medium (as control) was then subcutaneously placed on the dorsal side of the animals. A pocket was created under the skin at the level of the shoulder blades for device insertion, followed by closure of the skin wound. On obtaining spontaneous respiration, a single dose of carprofen (5 mg/kg, subcutaneous injection) was administered for analgesia. Sham control rats underwent similar open chest surgery without coronary artery occlusion. Animals were randomly assigned to experimental groups. At the end of the 12-week reperfusion period, following the final echocardiographic assessment, rats were maintained under deep anaesthesia and humanely euthanized by surgical removal of the heart.

Part 2 validation study: Male and female Sprague Dawley rats, aged 51–53 weeks, were placed on a high fat rodent diet (total digestible energy: 60.8% lipids, 18.4% protein, and 88.9 g/Kg sucrose; Specialty Feeds; SF13-092). After four weeks, the rats underwent either

myocardial ischaemia-reperfusion injury or sham operation (as described above), while continuing the high fat diet for 12 weeks. At the time of reperfusion, a Procyon device containing either 4×10^6 Cymerus MSCs or serum-free expansion medium (control) was subcutaneously implanted on the dorsal side of the animals. Animals were randomly assigned to experimental groups. At the end of the 12-week reperfusion period, following the final echocardiographic assessment, rats were maintained under deep anaesthesia and humanely euthanized by surgical removal of the heart.

Simulated IRI (in vitro)

Engineered cardiac microtissues were subjected to 3 h of hypoxia followed by 24 h of reoxygenation to model IRI. Hypoxia was induced in a hypoxic chamber (STEMCELL Technologies) using an ischemia-mimicking buffer, and reoxygenation was achieved by replacing the buffer with spheroid medium under normoxic culture conditions. Normoxic controls were maintained in spheroid medium throughout. At reoxygenation, microtissues were randomly assigned to receive either concentrated Cymerus MSC serum-free expansion medium (as vehicle control) or concentrated conditioned media of Cymerus MSCs at reoxygenation for 24 h.

Mass spectrometry-based proteomics

Proteomic analysis was performed on encapsulated Cymerus MSCs (cell lysates), their secretome (conditioned media), 2D Cymerus MSC monolayers, and human iPSCs. Protein lysates were prepared in 1% (v/v) sodium dodecyl sulphate (SDS) containing 50 mM HEPES (pH 8.0) and HALT protease and phosphatase inhibitor, homogenized by tip-probe sonication, and quantified by microBCA (Thermo Fisher Scientific) [14]. Cell and secretome samples (10 µg protein) were reduced and alkylated as previously described [37]. Briefly, samples were processed using the SP3 protocol [15], and digested with Trypsin and Lys-C (1:50 and 1:100 enzyme-to-protein ratios) overnight at 37 °C. Peptides were acidified to 2% formic acid, vacuum-lyophilized, reconstituted in 0.07% TFA, and quantified fluorometrically. LC-MS data acquisition was performed on a Q Exactive HF-X Orbitrap mass spectrometer coupled with UltiMate™ NCS-3500RS nano-HPLC, operated with Xcalibur software [14, 16].

Biological replicates included encapsulated Cymerus MSCs pre-implantation (n = 2), post-implantation/ex vivo cultured (n = 3), 2D MSCs (n = 2), and iPSCs (n = 3). DIA-MS spectra were processed using DIA-NN v1.9 [17] against the human proteome database (UP000005640, 83,401 entries) as previously reported [14, 18]. Data were analysed with Perseus v2.0.11 for log2 transformation, quantile normalization, PCA, and statistical testing (unpaired Student's t-test or Welch's t-test with missing values imputed from normal distribution, width = 0.3, downshift = 1.8). Functional enrichment and pathway analyses were performed with g: Profiler and Reactome ($P < 0.05$). MS proteomics data were deposited into the ProteomeXchange Consortium via the MassIVE partner repository and are available via MassIVE under the identifier MSV000097257.

Statistics

Data are expressed as mean ± standard error of the mean (SEM) with three significant figures. Statistical significance of differences was evaluated using Student's or Welch's t-test, or one-way or two-way ANOVA followed by Tukey's multiple comparison post hoc analysis where appropriate. A $P < 0.05$ was considered statistically significant.

Results

Subcutaneously implanted Cymerus MSCs in Procyon device protects young rats from chronic myocardial ischaemia-reperfusion injury

To assess the therapeutic effect of Cymerus MSCs on myocardial ischaemia-reperfusion injury, the Procyon device containing Cymerus MSCs was subcutaneously implanted at reperfusion after coronary artery ligation. Pre-operative echocardiography showed no differences in cardiac function among the groups. Following chronic myocardial ischaemia-reperfusion injury, immunocompetent young rats exhibited a progressive deterioration in cardiac function over the 12-week reperfusion period (Fig. 1A). However, treatment with Cymerus MSCs encapsulated within the Procyon immunoisolation device significantly preserved cardiac function, showing a significant improvement in ejection fraction at a dose of 4×10^6 cells by 12 weeks following ischaemia-reperfusion injury (59.9 ± 0.853% versus 49.3 ± 1.98% in control, $P < 0.05$, Fig. 1B). The improvement in cardiac function was associated with reductions in cardiac hypertrophy (Fig. 1C), cardiomyocyte hypertrophy (Fig. 1D), infarct scar size (Fig. 1E), and interstitial fibrosis (Fig. 1F), while the myocardial vascular density was similar among groups (lectin$^+$/mm^2 = 2470 ± 77.7 in Sham, 2140 ± 60.3 in Control, 2310 ± 81.7 in 1×10^6 Cymerus MSCs, 2190 ± 150 in 2×10^6 Cymerus MSCs, and 2270 ± 44.1 in 4×10^6 Cymerus MSCs; $P > 0.05$, n = 4–6).

Cardioprotective efficacy in aged and metabolically stressed male and female rats

To further validate the cardioprotective effects of Cymerus MSCs in a clinically relevant model, immunocompetent, middle-aged male and female Sprague-Dawley rats were utilized. These rats were fed a high-fat diet and subjected to chronic myocardial

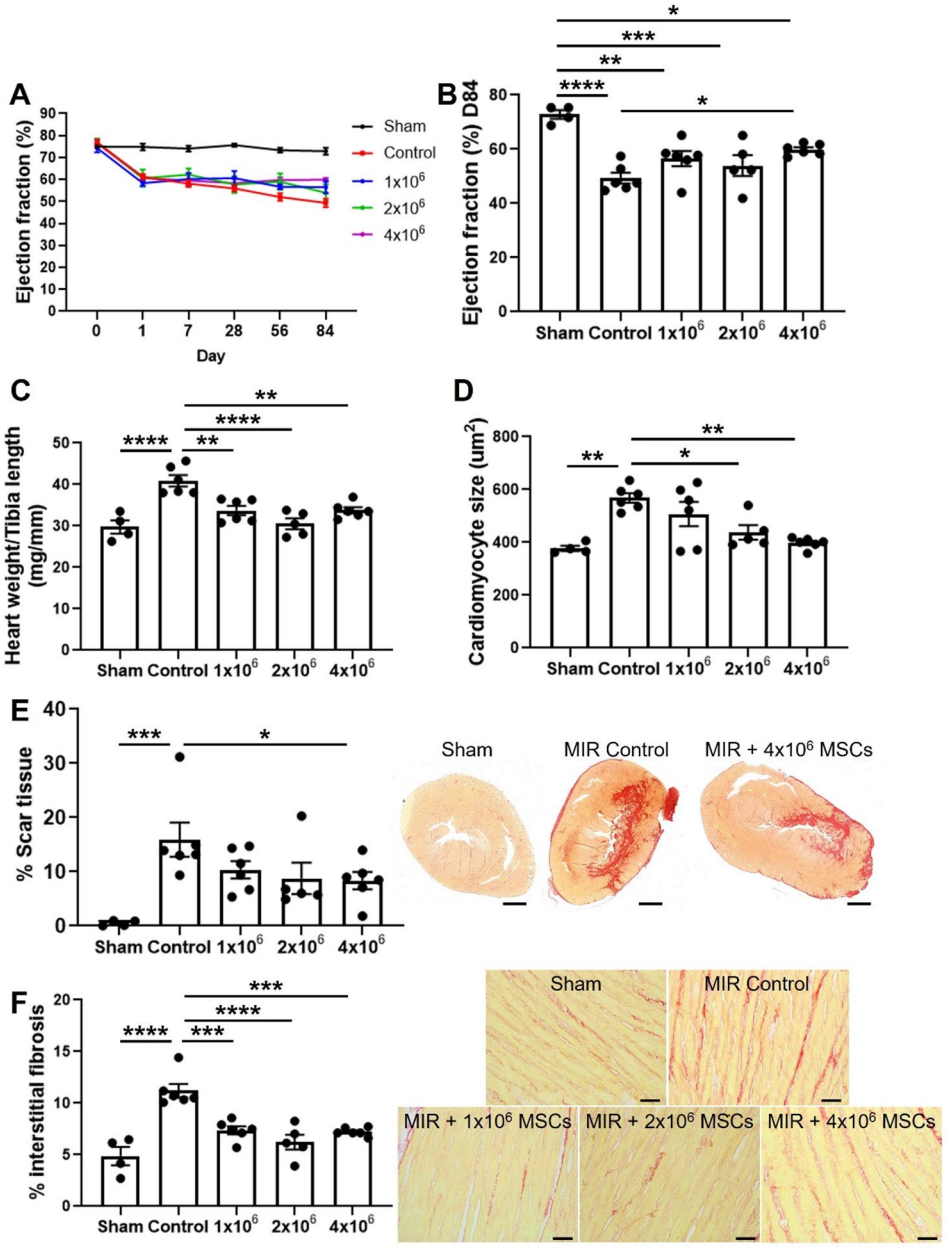

Fig. 1 Cardioprotective effects of Cymerus MSCs encapsulated within a Procyon immunoisolation device in young rats following chronic myocardial ischaemia-reperfusion injury. **A** Changes in the left ventricular ejection fraction from baseline over a 12-weeks of reperfusion period. **B** Changes in the left ventricular ejection fraction on day 84 (D84) following chronic myocardial ischaemia-reperfusion injury. **C**–**F** Cardiac structural and histological assessments on day 84 following chronic myocardial ischaemia-reperfusion injury: **C** normalised heart weight, **D** relative cross-sectional area of cardiomyocytes, **E** infarct scar size expressed as the percentage of fibrotic scar area over total left ventricle and representative cross-sectional images of myocardium stained with picrosirius red (scale bar = 2 mm), and **F** percentage of interstitial fibrosis in the remote myocardium and representative cross-sectional images of myocardium stained with picrosirius red (scale bar = 50 µm). $n = 4$–6 rats. Data are presented as mean ± SEM. *$P < 0.05$, ***$P < 0.001$, ****$P < 0.0001$ by one-way ANOVA with Tukey post hoc test

ischaemia-reperfusion injury to mimic an AMI patient with common comorbidities of aging and metabolic stress. At the start of the study (ages 50–52 weeks), female rats exhibited lower body weights than male rats, a difference that remained consistent throughout the study period. Over the 108-day period of high-fat diet feeding, all rats showed weight gain regardless of sex, with no significant differences between treatment groups. While female rats consistently maintained lower overall body weights compared to males, the rate of weight gain was similar across all groups (Table 1).

Table 1 Body weight and blood biochemical values of aged rats

Experimental groups	Male			Female		
	Sham	IR	IR + Cymerus	Sham	IR	IR + Cymerus
Sample size	6	7	7	7	7	7
Body weight (g), day − 28 (before commencing HFD)	680 ± 49.5	677 ± 32.7	711 ± 26.2	441 ± 21.6	406 ± 22.5	396 ± 28.6
Body weight (g), day 0	775 ± 49.3	757 ± 39.0	775 ± 26.0	502 ± 24.4	459 ± 33.0	453 ± 36.4
Body weight (g), day 28	772 ± 49.1	744 ± 33.7	758 ± 25.5	497 ± 26.1	442 ± 31.0	425 ± 33.9
Body weight (g), day 56	794 ± 45.9	770 ± 37.3	799 ± 29.4	524 ± 21.8	478 ± 38.7	458 ± 39.6
Body weight (g), day 84	804 ± 49.3	789 ± 40.8	819 ± 29.1	554 ± 22.5	496 ± 47.3	497 ± 48.0
Blood glucose (mmol/L), day − 28 (before commencing HFD)	6.42 ± 0.36	6.74 ± 0.18	6.80 ± 0.50	6.11 ± 0.18	6.93 ± 0.32	7.39 ± 0.19
Blood glucose (mmol/L), day 0	7.73 ± 0.41	8.64 ± 0.49	8.50 ± 0.43	7.47 ± 0.46	7.79 ± 0.19	7.64 ± 0.23
Blood glucose (mmol/L), day 28	9.22 ± 0.29	9.06 ± 0.48	8.93 ± 0.47	9.24 ± 0.45	8.04 ± 0.32	8.59 ± 0.42
Blood glucose (mmol/L), day 56	8.42 ± 0.17	8.41 ± 0.31	9.19 ± 0.81	9.07 ± 0.22	8.77 ± 0.25	8.55 ± 0.52
Blood glucose (mmol/L), day 84	9.97 ± 0.45	9.24 ± 0.84	10.77 ± 0.83	9.06 ± 0.62	9.89 ± 0.43	8.86 ± 0.51$^{\#}$
†HbA1C (%)	3.96 ± 0.11	3.92 ± 0.13	3.95 ± 0.08	3.87 ± 0.10	3.55 ± 0.07	3.75 ± 0.10
†Total cholesterol (mmol/L)	2.72 ± 0.29	2.57 ± 0.12	2.47 ± 0.18	2.18 ± 0.17	1.88 ± 0.18	1.94 ± 0.10
†Triglyceride (mmol/L)	1.70 ± 0.15	1.64 ± 0.16	2.14 ± 0.22	2.22 ± 0.31	2.27 ± 0.41	1.81 ± 0.25
†HDL (mmol/L)	1.76 ± 0.16	1.63 ± 0.08	1.61 ± 0.15	1.65 ± 0.11	1.47 ± 0.10	1.48 ± 0.09
†LDL (mmol/L)	0.65 ± 0.12	0.51 ± 0.04	0.45 ± 0.08	0.17 ± 0.02$^{\#\#\#\#}$	0.13 ± 0.02$^{\#\#}$	0.13 ± 0.01$^{\#\#}$
†CRP (pg/mL)	1280 ± 203	2630 ± 898	1440 ± 228	2220 ± 666	5700 ± 1960	677 ± 102**
†IL-6 (pg/mL)	500 ± 263	398 ± 175	180 ± 59.8	611 ± 207	395 ± 62.9	152 ± 34.2
†IL-1β (pg/mL)	62.5 ± 18.7	69.1 ± 24.6	66.5 ± 35.2	67.7 ± 14.8	63.2 ± 11.8	44.2 ± 9.16
†TNFα (pg/mL)	15.6 ± 4.34	18.2 ± 5.49	17.9 ± 8.80	19.6 ± 4.38	17.6 ± 3.06	12.0 ± 2.03

†Measurements were performed on day 84 endpoint. HFD (high fat diet), HDL (high-density lipoprotein), LDL (low-density lipoprotein), CRP (c-reactive protein), IL (interleukin), TNFα (tumor necrosis factor-alpha)

$^{\#}P < 0.05$, $^{\#\#}P < 0.01$, $^{\#\#\#\#}P < 0.0001$ versus male cohort of the same treatment group, and $^{**}P < 0.01$ versus female IR group by one-way ANOVA with Tukey post hoc test

Blood glucose concentrations were elevated in both male and female rats after 108 days on the high-fat diet, with no significant differences between sexes or treatment groups, except that female rats treated with Cymerus MSCs had lower blood glucose concentrations than their male counterparts (Table 1). Other blood biochemical markers, such as total cholesterol, triglyceride and high-density lipoprotein, were generally comparable across sexes and groups, except for low-density lipoprotein levels, which were significantly lower in female rats than in males (Table 1). This model effectively simulates metabolic stress, and comorbidity risks common in middle-aged AMI patients, providing a clinically relevant preclinical framework for assessing the cardioprotective efficacy of Cymerus MSCs.

Following myocardial ischaemia-reperfusion injury, middle-aged male and female rats displayed a progressive decline in cardiac function over the 12-week reperfusion period (Fig. 2A). However, treatment with Cymerus MSCs encapsulated within the Procyon immunoisolation device significantly preserved cardiac function in this pre-clinical animal model. By 12 weeks following ischaemia-reperfusion injury, both male and female rats showed significant improvement in ejection fraction (Fig. 2A-B), with effects like those observed in younger rats (Fig. 1). This improvement was accompanied by significant attenuation of adverse cardiac remodelling, including reductions in cardiac hypertrophy (Fig. 2C), cardiomyocyte hypertrophy (Fig. 2D, Supplementary Figure S1), infarct scar size (Fig. 2E, Supplementary Figure S1), and interstitial fibrosis (Fig. 2F, Supplementary Figure S1). Similar to younger male rats, myocardial vascular density in the remote myocardium was comparable among groups in middle-aged male rats (2770 ± 214 lectin^{+}/mm^{2} in Sham, 2450 ± 86.8 lectin^{+}/mm^{2} in Control, and 2910 ± 130 lectin^{+}/mm^{2} in Cymerus MSCs, $P > 0.05$, $n = 6$–7). Interestingly, in middle-aged female rats, myocardial vascular density was significantly higher in the Cymerus MSC-treated group compared to the control group (3060 ± 183 lectin^{+}/mm^{2} in Cymerus MSCs versus 2410 ± 158 lectin^{+}/mm^{2} in Control, $P < 0.05$, $n = 7$). Analysis of inflammatory cytokine levels at 12 weeks following ischaemia-reperfusion injury showed an increase levels of the inflammatory marker CRP, though it did not reach statistical significance. Treatment with Cymerus MSCs reduced CRP levels, achieving statistical significance in female rats. Additionally, Cymerus MSCs reduced inflammatory cytokines IL-6 and TNFα, with a stronger effect observed in female rats (Table 1). These results underscore the robust therapeutic potential of Cymerus MSC treatment across age groups and sexes.

Post-implantation morphological adaptations of Cymerus MSCs

To evaluate the effects of in vivo implantation on Cymerus MSCs, we performed histological analysis on

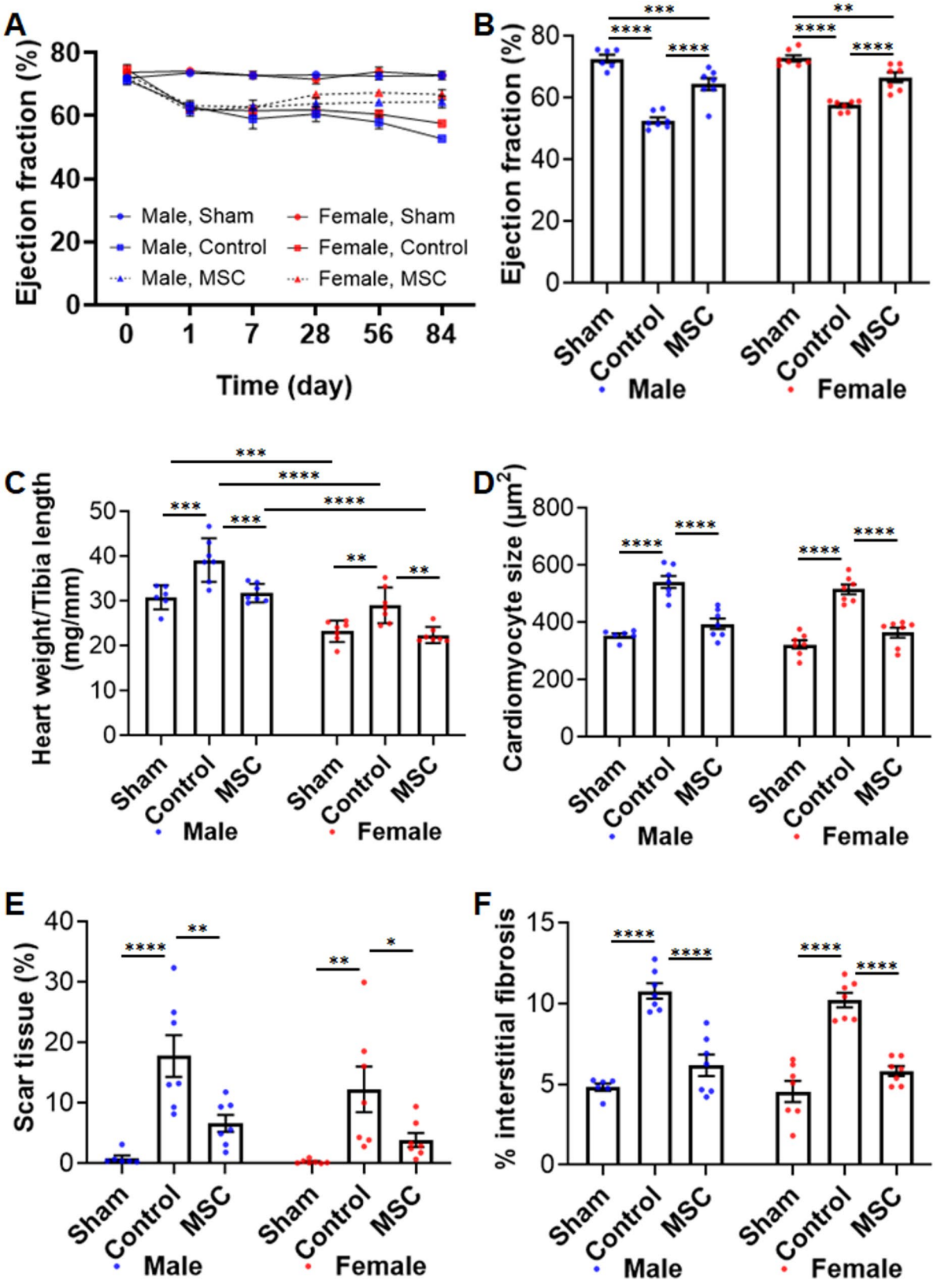

Fig. 2 (See legend on next page.)

(See figure on previous page.)

Fig. 2 Cardioprotective effects of Cymerus MSCs encapsulated within a Procyon immunoisolation device in middle-aged male and female rats following chronic myocardial ischaemia-reperfusion injury. **A** Changes in the left ventricular ejection fraction from baseline over a 12-weeks of reperfusion period. **B** Changes in the left ventricular ejection fraction on day 84 following chronic myocardial ischaemia-reperfusion injury. **C**–**F** Cardiac structural and histological assessments on day 84 following chronic myocardial ischaemia-reperfusion injury: normalised heart weight (C), relative cross-sectional area of cardiomyocytes in the remote myocardium (**D**), infarct scar size expressed as the percentage of fibrotic scar area over total left ventricle (**E**), and percentage of interstitial fibrosis in the remote myocardium (**F**). $n = 6$–7 rats. Data are presented as mean ± SEM. *$P < 0.05$, **$P < 0.01$, ***$P < 0.001$, ****$P < 0.0001$ by one-way ANOVA with Tukey post hoc test across both sexes

Procyon devices retrieved 12 weeks after subcutaneous implantation in immunocompetent rats. Human-specific KU80 staining confirmed that encapsulated Cymerus MSCs remained fully contained within the inner membranes of the devices (Supplementary Figure S2). The encapsulated cells appeared viable, exhibiting well-preserved morphology with intact membranes and clearly defined nuclei, and showed no signs of apoptosis, as indicated by the absence of cleaved caspase-3 (Fig. 3A-B, Supplementary Figure S2).

Similar to the control device (lacking encapsulated Cymerus MSCs), minimal leukocyte infiltration was observed around the devices containing Cymerus MSCs at 12 weeks post-implantation, suggesting an absence of immunological or xeno-immune reactions toward the foreign material and cells (Fig. 3B). Over the 12-week period, the encapsulated cells continued to express stromal/mesenchymal marker vimentin and reorganized into tissue-like structures supported by self-secreted extracellular matrices within the devices (Fig. 3A-B, Supplementary Figure S2). Notably, cartilaginous tissue formation was detected in one of the 28 implanted devices, as evidenced by positive Alcian blue staining (Supplementary Figure S2). Immunostaining with the pan-cell cycle marker Ki67 revealed reduced proliferative activity of Cymerus MSCs at 12 weeks post-implantation compared with pre-implantation, with no evidence of cell death (Supplementary Figure S2). Additionally, extensive vascularization was observed along the outer membranes of the devices, with rodent-specific lectin staining indicating integration with the host vasculature (Supplementary Figure S2). These findings suggest that the encapsulated Cymerus MSCs retained structural integrity and viability while forming organized tissue structures within the device. Further, proliferative activity of encapsulated MSCs declines over time, and the outer membrane matrix promoted robust vascularization, enhancing host-device integration.

Proteomic profile of encapsulated Cymerus MSCs following in vivo implantation

To better understand the temporal cellular changes in Cymerus MSCs during implantation, a global (untargeted) proteomic analysis was performed on encapsulated Cymerus MSCs both before implantation and 12 weeks post-implantation. Using stringent identification criteria, 3356 proteins were identified in pre-implantation phase, and 1782 proteins in post-implantation (Supplementary Table 1, Supplementary Figure S3A). Principal component analysis revealed distinct clustering of encapsulated Cymerus MSCs, including their relation to human iPSC proteome (Fig. 3C, Supplementary Table 1).

Conserved proteome following encapsulation

Cymerus MSCs retained a conserved core cellular proteome following encapsulation within the immunoisolation devices. When comparing monolayer cultured MSCs (2D MSC) to encapsulated MSCs pre-implantation (MSC-Pre), minimal impact on the cellular proteomic profile was observed, with 3,357 proteins commonly identified based on abundance/identification (>75% of cellular proteome) (Supplementary Figure S3B-E, Supplementary Table 2). Key MSC markers within this subset include NCAM1, ANPEP, MME, THY1 (CD90), ALCAM, ITGB1 (CD29), NT5E (CD73), MCAM, PDGFRB, SRC, ENG (CD105), and CD44. Of the 475 proteins with altered expression associated with encapsulation, enrichment was observed in biological process ontologies related to cell adhesion (HAS1, LAMC1, LAMB1, CBFB), extracellular matrix organization (HAS1, COL1A2, LAMC1, ERO1A), wound healing (CLIC1, VKORC1, AK3, TOR1A, MYL12A), and collagen metabolism (COL1A2, CTSB, MMP14, MRC2, FAP) (Supplementary Tables 3–4, Supplementary Figure S3E).

Proteomic changes in the cellular landscape post-implantation

To compare cellular proteome landscape of encapsulated Cymerus MSCs pre (MSC-Pre) and post-implantation (MSC-Post), a global analysis was performed to identify changes that reflected the proteome environment of the in vivo implant. Of the 1547 proteins commonly identified (43.1% of the Cymerus MSC cellular proteome containing 3591 proteins, Supplementary Table 5), key biological processes were enriched, including extracellular vesicle dynamics (RAB11B, RAB15, RAC1, CDC42, ARPC2, TOLLIP, MVP), extracellular matrix organization (LAMA4, COL3A1, MMP2, HAPLN1, COL11A1), tissue development (EGFR, TGFBI, AKT1, FN1, POSTN, MAPK3), angiogenesis (NRP1, AKT1, RRAS, LOXL2), antioxidant activity (PRDX5, PRDX4, GPX7, CP, APOE), response to endogenous stimulus (EGFR, ANXA1, SERPINF1, GSTM3, CAV1), cell death regulation (AKT1, PRKAA1, MAPK3, CLU), immune regulation protein

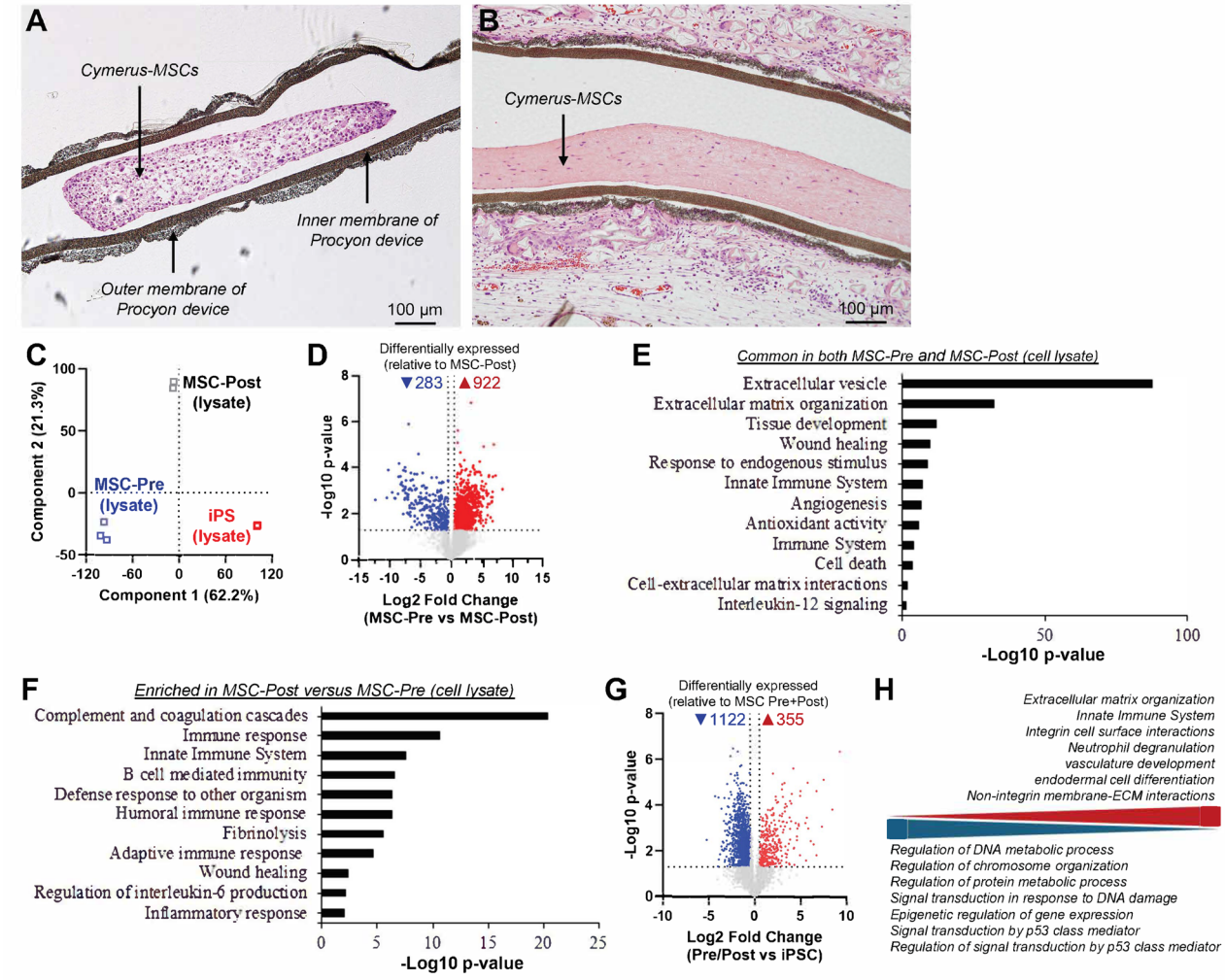

Fig. 3 Morphological and proteomic network changes in encapsulated Cymerus MSCs following in vivo implantation in rats subjected to chronic myocardial ischaemia-reperfusion injury. **A**, **B** Haematoxylin and eosin stained cell encapsulated Procyon device at 0 (**A**, Pre) and 12 (**B**, Post) weeks post-implantation. **C–H** Global proteome analysis of encapsulated Cymerus MSCs at 0 (MSC-Pre) and 12 (MSC-Post) weeks post-implantation, and human iPSCs. **C** Principal component analysis of indicated cellular proteomes. **D** Volcano plot of cellular proteome of MSC-Pre relative to MSC-Post, based on Welch's T-Test, $P < 0.05$ and log2 fold change of 0.5. Functional enrichment analysis of Reactome and GO networks/terms enriched ($P < 0.05$) in proteins commonly identified and expressed in MSC-Pre and MSC-Post cellular proteome (**E**), and in proteins significantly upregulated in expression in MSC-Post cellular proteome relative to MSC-Pre cellular proteome (**F**). **G** Volcano plot of cellular proteome of encapsulated Cymerus MSCs (MSC-Pre and MSC-Post combined) relative to iPSCs. Based on Welch's T-Test, $P < 0.05$ and log2 fold change of 0.5. **H** Trend enrichment analysis of Reactome networks and GO biological processes. Biological process enriched ($P < 0.05$) in differentially expressed Cymerus MSC (MSC-Pre and MSC-Post combined) relative to iPSC cellular proteome

networks (ACTB, HP, ANPEP, RAC2, CD44), membrane trafficking (ACTB, EGFR, MAN1A1, DAB2, COPZ2), interleukin-12 signalling (CDC42, RAP1B, P4HB, MIF, ANXA2), and cell-extracellular matrix interactions (ACTB, LIMS2, LIMS1, ILK, PARVA). Notably, MSC markers CD44 and vimentin (VIM) were also identified (Fig. 3E, Supplementary Table 6). While reduced Ki67 expression was detected in encapsulated Cymerus-MSCs at 12 weeks post-implantation (Supplementary Figure S2), proteomic analysis did not detect common senescence-associated proteins, including p16INK4a (CDKN2A), p21CIP1 (CDKN1A), p53 (TP53), 53BP1 (TP53BP1), or γH2AX (H2AX) (Supplementary Fig. 1, Supplementary Fig. 7).

A subset of 179 proteins (5.0% of the total cellular proteome) were uniquely identified in the post-implant cell proteome, associated with immune effector processes (IGKV3-15, IGHV3OR16-12, IGHV1OR15-1, IGHV1-45, IGKV6D-21, NEDD4), anti-inflammatory responses (LGALS9, A2M, PTPN6, IRF5, IKBKG), complement activation (C4A, C3, F13A1, F2, C1R, PLG), wound healing (F13A1, F2, PLG, FGA, FGB), and fibrinolysis (FGG, VTN, CPB2) (Fig. 3F, Supplementary Table 7). Together, these findings suggest that MSCs undergo proteome

reprogramming upon implantation to adapt to the in vivo environment, promoting immune modulation, tissue repair, and integration into the surrounding tissue.

To further understand MSC proteome reprogramming relative to their iPSC origin, Welch's T-Test paired analyses identified 355 conserved MSC-associated proteins in both MSC-Pre and MSC-Post (Fig. 3G, Supplementary Table 5). These proteins were enriched in key biological processes, including extracellular matrix organisation, innate immune function, integrin cell surface interactions, collagen formation, and vasculature development (Fig. 3H, Supplementary Table 8). In contrast, 1122 proteins were significantly enriched in iPSCs compared to MSCs, primarily associated with cell cycle regulation, DNA metabolism, chromosome organisation, epigenetic regulation of gene expression, and p53-mediated signalling (Fig. 3G-H, Supplementary Tables 5 and 9). This comparison highlights how MSCs and iPSCs are specialised at the cellular proteome level for their respective biological functions. MSCs are primed to maintain tissue homeostasis and respond to injury or inflammation, while iPSCs maintain pluripotency and the potential to differentiate into various cell types, a key characteristic of stem cell biology.

Adaptive response of Cymerus MSCs secreting factors implicated in cardiac biology and tissue remodelling post-implantation

Proteome profiling was performed to characterise the secretome composition of Cymerus MSCs and assess temporal changes in their secreted protein profile following in vivo implantation (ex vivo cultured). A total of 448 secreted proteins were identified (in at least one sample, and 69 proteins in at least two) from MSC-Pre, and 815 proteins (589 proteins in at least two samples) from MSC-Post (Fig. 4A, Supplementary Table 10). The encapsulation of Cymerus MSCs minimally affects their secretome when compared to Cymerus MSCs cultured in a monolayer (Supplementary Figure S4). Principal component analysis demonstrated a distinct clustering pattern

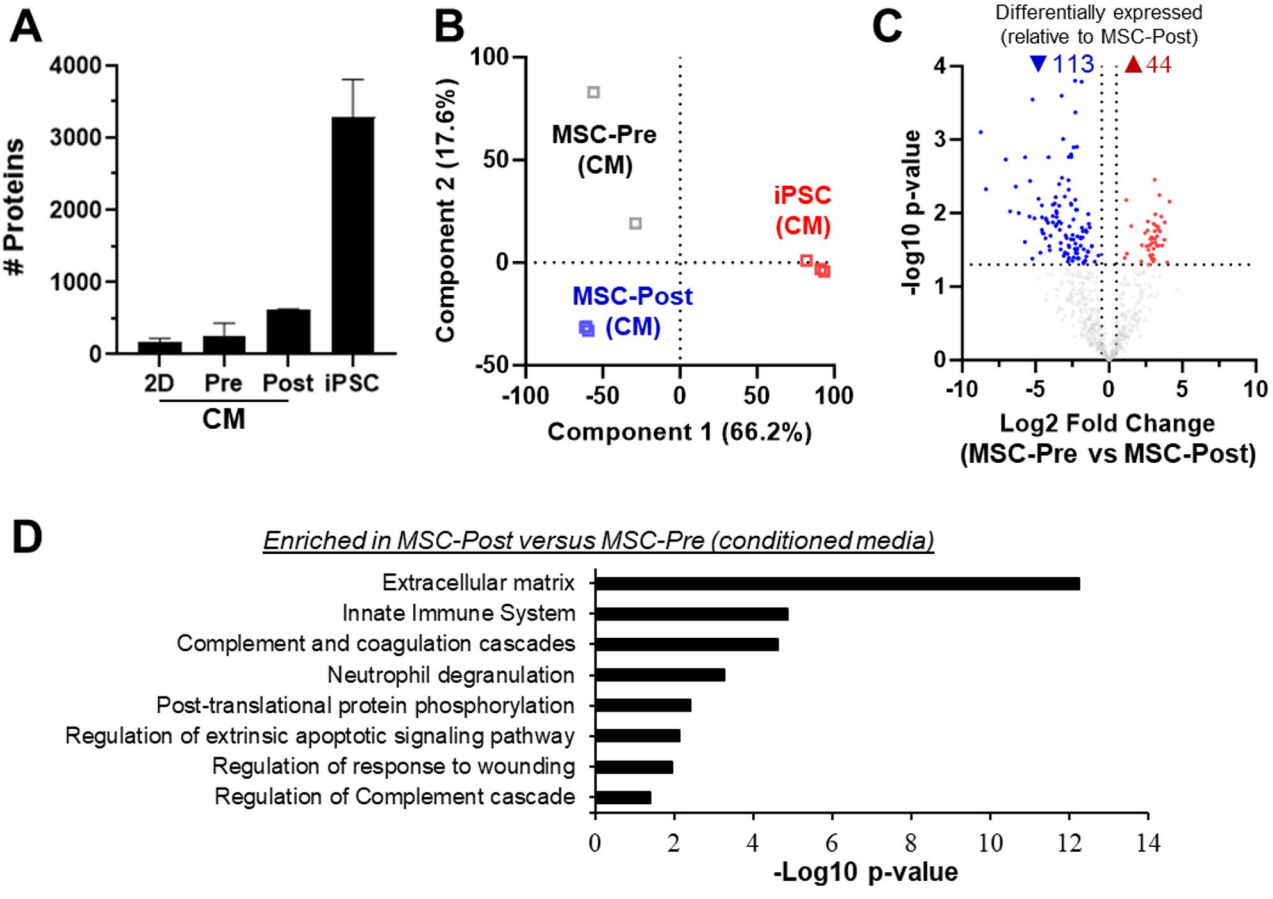

Fig. 4 Proteomic network changes in secretome of encapsulated Cymerus MSCs following in vivo implantation in rats subjected to chronic myocardial ischaemia-reperfusion injury. **A** Quantitative proteomic profiling reveals in-depth coverage and identified protein in conditioned media (CM) collected from 2D Cymerus MSC (2D), encapsulated Cymerus MSCs at 0 (MSC-Pre) and 12 (MSC-Post) weeks post-implantation, and human iPSCs. **B** Principal component analysis of indicated conditioned media (secretome) of Cymerus MSCs and human iPSC proteome. **C** Volcano plot of conditioned media proteome of MSC-Pre relative to MSC-Post. Based on Welch's T-Test, $P < 0.05$ and log2 fold change of 0.5. **D** Functional enrichment analysis of Reactome and GO networks/terms enriched ($P < 0.05$) in proteins significantly upregulated in expression in MSC-Post secretome relative to MSC-Pre secretome

in the MSC-Post secretome, indicating significant shifts in protein expression post-implantation (Fig. 4B).

While MSC markers CD44 and VIM were detected in both MSC-Pre and MSC-Post secretomes (Supplementary Table 11), a greater number of distinct proteins were identified in the secretome from the MSC-Post group compared to the MSC-Pre group (Fig. 4C). Functional enrichment analyses of this protein subset revealed pathways associated with the innate immune system (ITIH3, ARHGDIA, ANXA1, SUMO2, PLG), extrinsic apoptosis (FGG, FGB, SERPINE1), extracellular matrix synthesis (ANXA1, MRC2, VCAN), complement cascade (SUMO2, SYNCRIP, RAD23B), neutrophil degranulation (ANXA1, PLG, LTA4H), and response to wounding (FGG, FGB, ANXA1, PLG, SERPINE1) (Fig. 4D, Supplementary Tables 12 and 13). This analysis highlighted an enrichment of secreted proteins in the MSC-Post group (relative to MSC-Pre) associated with wound repair, protection, inflammation, immune regulation, and tissue remodelling.

To further investigate Cymerus MSC secretome reprogramming in relation to encapsulated states (both pre- and post-implantation) and iPSC secreted profiles, a Welch's T-Test was performed. This identified significant differences between Cymerus MSC and iPSC secretomes, with 58 proteins enriched and 193 downregulated in Cymerus MSC relative to iPSC (Supplementary Table 14). iPSC secretome enrichment includes biological processes and pathway networks associated with RNA metabolism, cap-dependent translation, cell cycle, protein metabolism, RNA degradation, and DNA replication pathways (Supplementary Table 15). In contrast, the Cymerus MSC secretome is enriched in ECM processes, extracellular vesicles, and oxidant detoxification (Supplementary Table 16). These findings suggest that Cymerus MSCs undergo significant reprogramming in response to in vivo implantation, with distinct changes in their secretome profile that may contribute to their therapeutic potential.

Cardioprotective effect of Cymerus MSC secretome in a human engineered cardiac microtissue model of ischaemia-reperfusion injury

To assess the cardioprotective effect of Cymerus MSC secretome in a human context, we generated engineered cardiac microtissues composed of human iPSC-derived cardiomyocytes, endothelial cells, vascular smooth muscle cells, and cardiac fibroblasts. Within these 3D engineered cardiac microtissues, cardiomyocytes self-organised into a ring-like structure, mimicking native cardiac tissue architecture. Endothelial cells localised around the lumen-like inner core, suggesting the formation of primitive vascular structures. Meanwhile, vimentin-positive mesenchymal stromal cells/fibroblasts and smooth muscle cells were distributed throughout the engineered cardiac microtissue and distributed among the cardiomyocytes, contributing to the structural complexity and cellular interactions necessary for functional cardiac tissue development (Fig. 5A).

Engineered cardiac microtissues subjected to simulated IRI showed a significant decrease in viability compared to the normoxia group. Treatment with Cymerus MSC secretome significantly improved the viability of engineered cardiac microtissues when compared to the IRI control group (Fig. 5B). Similarly, mitochondrial ROS levels were significantly elevated following simulated IRI but were significantly reduced with Cymerus MSC secretome treatment (Fig. 5C). We also assessed the contraction kinetics of the engineered cardiac microtissues, including time-to-peak contraction, relaxation time, and beat rate variability. Compared to the normoxia control, engineered cardiac microtissues exposed to simulated IRI showed a significantly prolonged total contraction duration, time-to-peak, and relaxation time. These changes were effectively prevented by Cymerus MSC secretome treatment (Fig. 5D-F). Beat rate variability remained consistent across all experimental groups (Fig. 5G). Under normoxic conditions, treatment with Cymerus MSC secretome had no impact on engineered cardiac microtissue viability, mitochondrial ROS production, or contraction kinetics compared to the normoxia control (Fig. 5B-G).

Discussion

This study presents an innovative strategy for secretome-based cardioprotection using human iPSC-derived MSCs delivered via the Procyon immunoisolation device. In an immunocompetent rat model of chronic myocardial ischaemia-reperfusion injury, this approach significantly improved cardiac function, reduced fibrosis, and demonstrated long-term therapeutic benefits. Furthermore, the cardioprotective effect of the MSC secretome remained effective in aged and metabolically stressed animals, comorbidities that typically compromise the efficacy of other cardioprotective strategies such as ischaemic conditioning and remote ischaemic preconditioning [19–21]. This is particularly significant, as many cardioprotective interventions fail to translate into clinical practice due to the prevalence of elderly patients with multiple comorbidities, a population often resistant to conventional treatments. The resilience of MSC secretome therapy under these challenging conditions presents a promising clinically applicable therapeutic avenue. Although the cardioprotective efficacy of Cymerus MSCs in clinical settings has yet to be determined, our data from human iPSC-derived engineered cardiac microtissues suggest their potential translatability to humans. These findings demonstrate significant protection against ischaemia-reperfusion injury, including restored

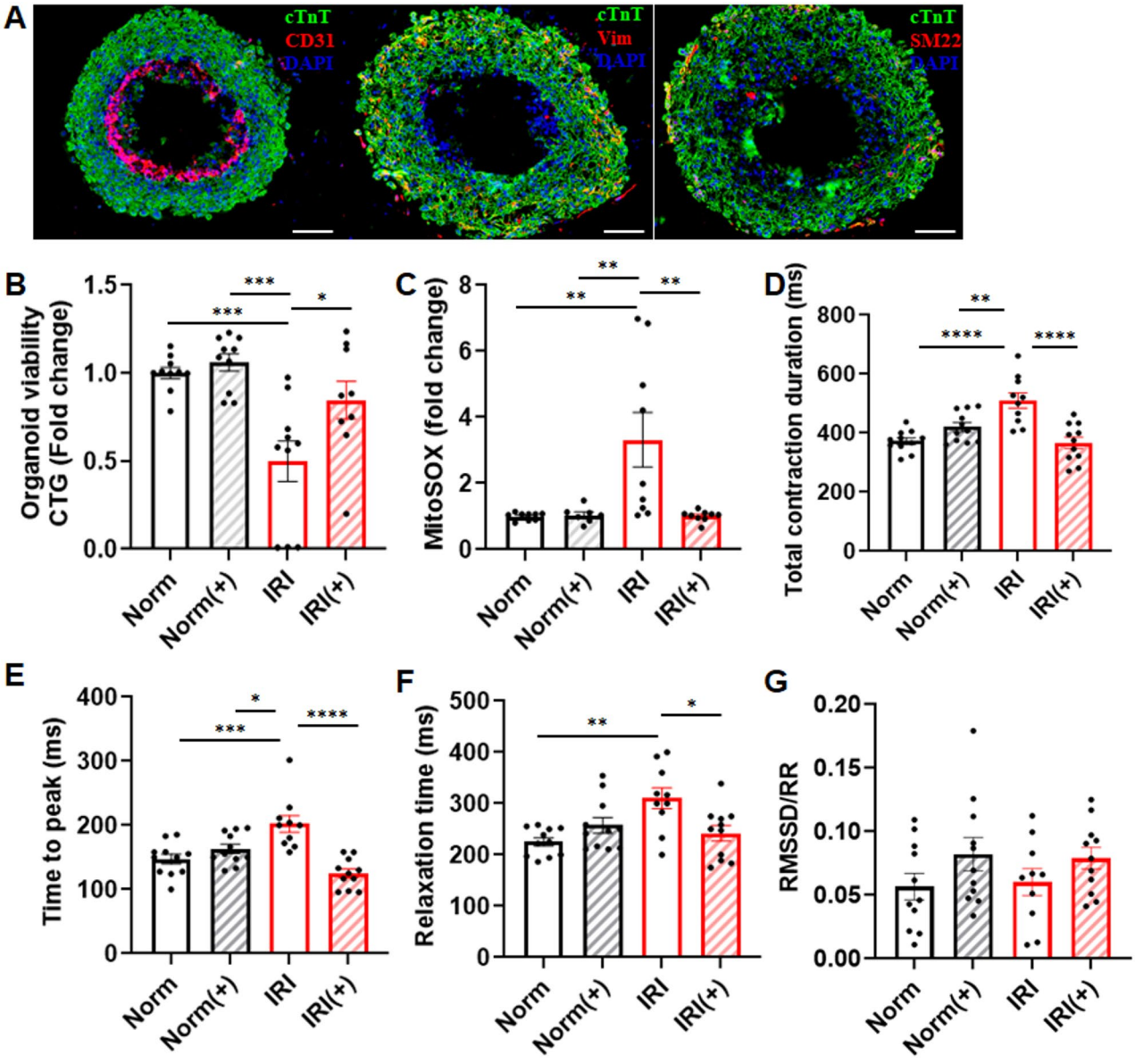

Fig. 5 Cardioprotective effects of Cymerus MSC secretome in a pre-clinical human engineered cardiac microtissue model of ischaemia-reperfusion injury. **A** Representative images of engineered cardiac microtissues stained with cardiac troponin T (cTnT, a marker for cardiomyocytes), CD31 (a marker for endothelial cells), SM22 (transgelin, a marker for smooth muscle cells) and vimentin (a marker for mesenchymal stromal cells and fibroblasts). Scale bar = 100 µm. **B** Viability of engineered cardiac microtissues assessed by CellTiter-Glo assay ($n = 9–10$). **C** Mitochondrial ROS production of engineered cardiac microtissues assessed by MitoSOX Red indicator ($n = 7–9$). **D**–**G** The contraction profile of engineered cardiac microtissues; total contraction duration (**D**), time-to-peak (**E**), relaxation time (**F**), and beat rate variability calculated by the root mean square of successive differences normalised by the R-R interval (**G**) ($n = 10–11$). Engineered cardiac microtissues were subjected to normoxia (Norm) or simulated IRI conditions (IRI) and treated with vehicle control or 1000 µg of Cymerus MSC conditioned media (+). Data are shown as mean ± SEM. *$p < 0.05$, **$p < 0.01$, ***$p < 0.001$, ****$p < 0.0001$ by one-way ANOVA with Tukey post-hoc test

contractile function, enhanced cell viability and reduced oxidative stress, underscoring the therapeutic potential of Cymerus MSCs. Nevertheless, further investigation using well-designed clinical trials is essential to establish their safety, effectiveness, and long-term benefits in real-world scenarios.

Meta-analyses of clinical trials consistently report strong safety profiles for MSCs, with minimal adverse events such as immune rejection [22, 23]. Previous clinical trials involving intravenous delivery of Cymerus MSCs showed no tumours or other safety concerns over a two-year follow-up period [12, 24]. Our proteomic analysis of both the encapsulated Cymerus MSCs and their secretome post-implantation revealed no expression of oncogenic protein markers or signs of oncogenic transformation. Laboratory studies further confirmed

that the MSC secretome does not promote the growth of human cancer cells in culture (Supplementary Figure S5). Beyond in vitro assessments, ex vivo post-mortem analysis provides additional evidence supporting the safety profile of this approach. Histomorphological examination of rats implanted with devices containing Cymerus MSCs showed no signs of tissue abnormalities or malignancy, supporting that this intervention does not promote a pro-tumorigenic environment. Together, these findings reinforce the safety profile of Cymerus MSCs, affirming their non-oncogenic properties, immune compatibility, and controlled biological activity. These attributes position them as a safe and viable option for regenerative medicine.

MSCs have gained significant attention in regenerative medicine for their potential to protect the heart in various pathological conditions, including myocardial infarction [6, 25]. The cardioprotective effects of MSCs are largely attributed to their paracrine signalling, where they secrete bioactive factors such as cytokines, growth factors, and extracellular vesicles that mediate their therapeutic actions. Rather than transdifferentiating into cardiomyocytes and directly replacing damaged heart cells, MSCs promote tissue repair by reducing arrhythmic risk, modulating inflammation, preventing apoptosis, limiting fibrosis, and promoting angiogenesis. These actions contribute to myocardial preservation and functional recovery following injury [4, 6, 26–28]. The paracrine mechanism of MSCs is evidenced by the observation that conditioned media derived from MSCs or cell extracts can exert cardioprotective effects comparable to those achieved by delivering live MSCs to the heart [27–31]. Our data further supports this paracrine effect, demonstrating cardioprotection when MSCs are delivered via an immunoisolation device implanted remotely from the myocardium [11]; suggesting that MSCs do not need to be in direct contact with the heart to exert their beneficial effects. Consistent with this, several studies have reported that pericardial, subcutaneous or remote MSC transplantation using hydrogels also confers cardiac protection, with outcomes largely attributed to paracrine/secretome release and immune modulation rather than direct cell engraftment [32–37]. These approaches highlight the systemic reach of MSC-derived factors, reinforcing the concept that therapeutic benefit does not strictly require intramyocardial delivery. Notably, while emerging cell delivery approaches using cell-encapsulating hydrogels aim to improve cell retention, their benefits are often short-lived, as most hydrogels biodegrade within weeks. In contrast, remote or subcutaneous MSC-based strategies, particularly when paired with durable immunoisolation platforms, provide a less invasive and more sustained therapeutic effect by enabling continuous secretome release. Future studies should investigate how immunoisolation device-based, secretome-centric strategies compare with other delivery methods, focusing on their potential to overcome the invasiveness and transient efficacy of hydrogel-based approaches while maintaining the cardioprotective effects of MSCs in a clinically translatable manner.

A recent study transplanting noncontractile cardiomyocytes further highlights the role of secretome-based cardioprotection, demonstrating that the cardiac benefits are primarily due to the secretion of paracrine factors, rather than cardiomyocyte graft contraction. In this study, engineered noncontractile human iPSC-derived cardiomyocytes, created by knocking out TNNI1 and TNNI3, were able to preserve cardiac function to a similar extent as contractile cardiomyocytes [38]. Interestingly, some studies have shown that transplanting dead or apoptotic stem cells into the heart can still provide cardioprotection [39]. More recent translational evidence, notably from Vagnozzi et al., indicates that the apparent benefits of cardiac cell therapy are largely mediated by an acute sterile inflammatory response rather than durable engraftment. In mice subjected to ischemia-reperfusion injury, intracardiac injection of live or dead stem cells, or even chemical inducers of innate immunity, triggered a regional accumulation of $CCR2^{+}$ and $CX3CR1^{+}$ macrophages, which modulated cardiac fibroblast activity, reduced extracellular matrix deposition in the border zone, and enhanced the mechanical properties of the injured myocardium [40]. This finding supports the "dying stem cell" [41] or "hit-and-die" [42] mechanism, in which transplanted cells exert transient paracrine effects and then die, stimulating endogenous reparative inflammation that improves cardiac function. Our findings extend these observations by demonstrating that remote, immunoisolated MSC delivery, where direct myocardial donor-cell death is precluded, can still confer robust cardioprotection. This approach highlights a distinct, secretome-centric pathway in which sustained release of MSC-derived factors, independent of acute inflammatory triggers, may provide a more targeted, controllable, and clinically translatable strategy for cardiac repair.

This underscores the resilience and therapeutic potential of MSC-mediated paracrine signalling, which can protect the myocardium even in the absence of cell engraftment or death. Future studies should focus on temporally profiling circulating secretome changes. For example, Cre-expressed models could be used to delineate discrete phases of the "dying stem cell" paradigm based on selective expression of modified proteins. In parallel, mapping cell-type-specific expression networks may help identify additional regulatory pathways that contribute to cardiac repair.

Optimising the therapeutic potential of Cymerus MSCs in cardiovascular disease requires a thorough

understanding of their cardioprotective mechanisms particularly their interaction with the host microenvironment. Their ability to sense ischaemic cues and secrete bioactive factors is central to their function, yet the precise nature of these interactions in pathological settings remains unclear. Investigating how transplanted MSCs adapt and modulate their secretome in response to host tissue signals will be key to refining their clinical application. Traditional delivery methods, such as intramyocardial or intravenous injection, present challenges in studying their in vivo behaviour, including the inability to retrieve transplanted cells and the difficulty of long-term tracking, as they are cleared from the host body within days [43–45]. The present study addresses this challenge by utilising encapsulated Cymerus MSCs, which can be retrieved post-implantation for detailed analysis. This approach provides significant insights into the dynamic reprogramming of MSCs in response to ischaemic injury, highlighting their substantial plasticity and therapeutic potential.

Following in vivo implantation, Cymerus MSCs showed significant proteomic shifts, with a significant increase in secreted proteins (589 post-implantation versus 69 pre-implantation) and distinct clustering patterns in principal component analysis. These changes enriched pathways involved in wound repair, immune regulation, and tissue remodelling. Additionally, post-implantation Cymerus MSCs demonstrated robust molecular reprogramming with 179 unique proteins linked to immune response, anti-inflammatory response, complement activation and wound healing. Their secretory profile shifted from pro-regenerative to immunomodulatory, in line with the inflammatory licensing process described by Hodgson-Garms and colleagues [46]. In this process, the resting MSCs primarily focussed on tissue homeostasis and repair, promoting extracellular matrix deposition and vascular development, with their secretomes rich in extracellular matrix and pro-regenerative proteins [4, 46, 47]. Under inflammatory conditions, such as myocardial infarction, these functions were downregulated, and MSCs prioritised the secretion of chemotactic and immunomodulatory proteins [46, 48]. Similarly, preconditioning with pro-inflammatory cytokines enhanced the anti-inflammatory and immunomodulatory properties of MSCs [49]. The reduced levels of inflammatory markers observed in plasma of rats treated with Cymerus MSCs, coupled with enhanced secretion of immunomodulatory factors [46, 47], further underscores their therapeutic potential. Future studies will be needed to further elucidate the immunomodulatory mechanisms underlying the effects of Cymerus-MSCs. In particular, profiling immune cytokine responses and characterising immune cell dynamics will provide deeper insight into how Cymerus-MSCs modulate post-infarction inflammation and contribute to cardiac repair. Collectively, these results emphasise the ability of Cymerus MSCs to modulate their secretome in response to environmental cues, providing new insights into their efficacy as regenerative therapies, particularly for cardiovascular diseases.

Several limitations of our study should be noted. First, although our proteomic analysis revealed a broad spectrum of MSC-mediated changes, it did not identify individual key proteins driving cardiac repair. Nevertheless, this approach captures the multifactorial and adaptive nature of the MSC secretome as a "living biodrug," modulating inflammation, fibrosis, oxidative stress, and other evolving pathologies. Second, the human engineered cardiac microtissue model only partially recapitulated clinical ischemia-reperfusion injury, lacking immune components and neuro-endocrine regulation, which may limit translation of some MSC effects. Finally, rare cartilage-like differentiation events likely reflect minor MSC plasticity without affecting therapeutic efficacy but warrant further investigation. Collectively, these limitations underscore the complexity of MSC-mediated cardiac repair and provide context for our findings.

In conclusion, MSCs primarily exert their cardioprotective effects through paracrine signalling, with their secretome driving therapeutic benefits. This shift supports secretome-based therapy as a less invasive and more efficient alternative to traditional direct cell transplantation. Despite extensive research, stem cell therapy for MI has yielded suboptimal outcomes due to the complex pathology of cardiovascular disease and poor cell retention. However, paracrine signalling is now widely recognized as the key mechanism behind MSC-driven cardiac repair. Our study highlights the advantages of encapsulated Cymerus MSCs, which remain viable post-implantation and continuously release therapeutic factors. This approach addresses key translational challenges, including histocompatibility concerns and poor engraftment, making MSC-secretome therapy a scalable and clinically viable strategy for long-term cardioprotection. Furthermore, this study provides valuable insights into the cellular reprogramming of Cymerus MSCs following in vivo implantation, revealing conserved and dynamic changes in their proteome that enhance their therapeutic potential for cardiovascular diseases. By deepening our understanding of the cellular and molecular mechanisms driving MSC-based therapies, this work paves the way for more effective and targeted clinical applications in regenerative medicine.

Supplementary Information

The online version contains supplementary material available at https://doi.org/10.1186/s13287-025-04847-9.

Supplementary Material 1.

Supplementary Material 2.

AI assistance disclosure
The authors declare that they have not use AI-generated work in this manuscript.

Author contributions
SYL conceived the project, designed, and performed the experiments, and analysed and interpreted data. AMK, DWG, JGL, AK, JC, AN, JP, SN, YD, LM, CK, TL, SYL planned and performed experiments, and analysed data. DWG, RHR, JM, KKP, KK, DH, TL, and SYL provided materials and methodologic input. DWG, JGL, JC, JRTD, TH, AN, JJHC, RHR, JLM, KKP, KK, DJH, TL, and SYL provided interpretative review of study findings. All authors participated in manuscript preparation and approved the final version of the manuscript.

Funding
This work was supported by the Medical Research Future Fund Cardiovascular Health Mission (2015523), St Vincent's Hospital (Melbourne) Research Endowment Fund and Stafford Fox Medical Research Foundation. DH is supported by the Duke-NUS Signature Research Programme funded by the Ministry of Health, Singapore Ministry of Health's National Medical Research Council under its Singapore Translational Research Investigator Award (MOH-STaR21jun-0003), Centre Grant scheme (NMRC CG21APR1006), and Collaborative Centre Grant scheme (NMRC/CG21APRC006), and CArdiovascular DiseasE National Collaborative Enterprise (CADENCE) National Clinical Translational Program (MOH-001277-01). The St Vincent's Institute of Medical Research and Baker Heart & Diabetes Institute receive Operational Infrastructure Support from the Victorian State Government's Department of Innovation, Industry and Regional Development.

Data availability
MS proteomics data were deposited into the ProteomeXchange Consortium via the MassIVE partner repository and are available via MassIVE under the identifier MSV000097257.

Declarations

Ethics approval and consent to participate
Cymerus™ MSCs were manufactured on behalf of the sponsor, Cynata Therapeutics Limited (https://cynata.com/), by Waisman Biomanufacturing (Madison, WI, USA). The iPSCs used to generate Cymerus™ MSCs were derived by Cellular Dynamics International (Madison, WI, USA) from peripheral blood mononuclear cells obtained from a healthy, fully consented adult donor, using a non-integrating, episomal-based reprogramming method, as previously described [50]. Donor material was collected by the BloodCenter of Wisconsin, Inc. under informed consent and in compliance with U.S. FDA donor eligibility regulations for Human Cells, Tissues, and Cellular and Tissue-Based Products (21 CFR 1271). Cynata Therapeutics Limited has confirmed that appropriate ethical approvals and informed donor consent were obtained for the collection and use of the human cells in accordance with applicable regulatory requirements [12]. The human iPS-Foreskin-2 cell line used in this study was originally derived and characterized by Yu et al. [13]. As described in the original publication, the line was generated from human neonatal foreskin fibroblasts obtained from a fully consented donor under protocols approved by the Institutional Review Board of the University of Wisconsin-Madison. The cells were provided to the authors as a gift from the originating laboratory, which confirmed that all necessary ethical approvals and informed donor consent were obtained for the collection and use of the human cells in research. All experimental procedures involving animal were approved by the Animal Ethics Committee of St Vincent's Hospital (AEC No. 011/22: Repairing the heart with clinical-grade human stem cells. Approval date 27 July 2022).

Competing interests
KK is an employee and shareholder of Cynata Therapeutics Limited. KKP is the co-founder and a stakeholder in Procyon Technologies LLC. TL holds a small ownership stake in Procyon Technologies LLC and is a member of its Scientific Advisory Board.

Author details
[1]St Vincent's Institute of Medical Research, Fitzroy, VIC 3065, Australia
[2]Department of Medicine and Surgery, University of Melbourne, Melbourne, VIC 3065, Australia
[3]Baker Heart and Diabetes Institute, Melbourne, VIC 3004, Australia
[4]Department of Cardiovascular Research, Translation and Implementation, La Trobe University, Melbourne, VIC 3086, Australia
[5]Baker Department of Cardiometabolic Health, University of Melbourne, Melbourne, VIC 3010, Australia
[6]Drug Discovery Biology, Monash Institute of Pharmaceutical Sciences, Monash University, Parkville, VIC 3052, Australia
[7]Early Origins of Adult Health Research Group, Health and Biomedical Innovation, Clinical and Health Sciences, University of South Australia, Adelaide, SA 5001, Australia
[8]Hearts4heart, Cheltenham, VIC 3192, Australia
[9]Department of Cardiothoracic Surgery, St Vincent's Hospital, Melbourne, VIC 3065, Australia
[10]Department of Cardiology, Westmead Hospital, Westmead, NSW 2145, Australia
[11]The Westmead Institute for Medical Research, The University of Sydney, Westmead, NSW 2145, Australia
[12]University of Toronto, The Hospital for Sick Children, Toronto, ON M5G 1X8, Canada
[13]Institute for Cellular Transplantation, Department of Surgery, University of Arizona College of Medicine-Tucson, University of Arizona, Tucson, AZ 85719, USA
[14]Procyon Technologies, LLC., Medical Research Building (Room 121), University of Arizona, Tucson, AZ 85718, USA
[15]Cynata Therapeutics Limited, Cremorne, VIC 3121, Australia
[16]The Hatter Cardiovascular Institute, Institute of Cardiovascular Science, University College London, 67 Chenies Mews, London WC1E 6HX, UK
[17]Cardiovascular and Metabolic Disorder Programme, Duke-NUS Medical School, Singapore 169857, Singapore
[18]Yong Loo Lin School of Medicine, National University Singapore, Singapore 119228, Singapore
[19]National Heart Research Institute Singapore, National Heart Centre, Singapore 169609, Singapore
[20]O'Brien Institute Department, St Vincent's Institute of Medical Research, 42 Fitzroy Street, Fitzroy, VIC 3065, Australia

Received: 22 June 2025 / Accepted: 27 November 2025
Published online: 05 December 2025

References

1. Wang Y, Li Q, Bi L, Wang B, Lv T, Zhang P. Global trends in the burden of ischemic heart disease based on the global burden of disease study 2021: the role of metabolic risk factors. BMC Public Health. 2025;25:310.
2. Swaroop G. Post-myocardial infarction heart failure: A review on management of drug therapies. Cureus. 2022;14:e25745.
3. Tompkins BA, Balkan W, Winkler J, Gyongyosi M, Goliasch G, Fernandez-Aviles F, Hare JM. Preclinical studies of stem cell therapy for heart disease. Circ Res. 2018;122:1006–20.
4. Thavapalachandran S, Le TYL, Romanazzo S, Rashid FN, Ogawa M, Kilian KA, Brown P, Pouliopoulos J, Barry AM, Fahmy P, Kelly K, Kizana E, Chong JJH. Pluripotent stem cell-derived mesenchymal stromal cells improve cardiac function and vascularity after myocardial infarction. Cytotherapy. 2021;23:1074–84.
5. Kawasumi R, Kawamura T, Yamashita K, Tominaga Y, Harada A, Ito E, Takeda M, Kita S, Shimomura I, Miyagawa S. Systemic administration of induced pluripotent stem cell-derived mesenchymal stem cells improves cardiac function through extracellular vesicle-mediated tissue repair in a rat model of ischemic cardiomyopathy. Regen Ther. 2025;28:253–61.
6. Han Y, Yang J, Fang J, Zhou Y, Candi E, Wang J, Hua D, Shao C, Shi Y. The secretion profile of mesenchymal stem cells and potential applications in treating human diseases. Signal Transduct Target Ther. 2022;7:92.
7. Guo Y, Yu Y, Hu S, Chen Y, Shen Z. The therapeutic potential of mesenchymal stem cells for cardiovascular diseases. Cell Death Dis. 2020;11:349.
8. Menasché P, Renault NK, Hagège A, Puscas T, Bellamy V, Humbert C, Le L, Blons H, Granier C, Benhamouda N, Bacher A, Churlaud G, Sabatier B, Larghero J. First-in-man use of a cardiovascular cell-derived secretome in heart failure: case report. eBioMedicine. 2024;103.

9. Golpanian S, Schulman IH, Ebert RF, Heldman AW, DiFede DL, Yang PC, Wu JC, Bolli R, Perin EC, Moye L, Simari RD, Wolf A, Hare JM. Cardiovascular cell therapy research N. Concise review: review and perspective of cell dosage and routes of administration from preclinical and clinical studies of stem cell therapy for heart disease. Stem Cells Transl Med. 2016;5:186–91.
10. Zhang J, Bolli R, Garry DJ, Marban E, Menasche P, Zimmermann WH, Kamp TJ, Wu JC, Dzau VJ. Basic and translational research in cardiac repair and regeneration: JACC State-of-the-Art review. J Am Coll Cardiol. 2021;78:2092–105.
11. Kompa AR, Greening DW, Kong AM, McMillan PJ, Fang H, Saxena R, Wong RCB, Lees JG, Sivakumaran P, Newcomb AE, Tannous BA, Kos C, Mariana L, Loudovaris T, Hausenloy DJ, Lim SY. Sustained subcutaneous delivery of secretome of human cardiac stem cells promotes cardiac repair following myocardial infarction. Cardiovasc Res. 2021;117:918–29.
12. Bloor AJC, Patel A, Griffin JE, Gilleece MH, Radia R, Yeung DT, Drier D, Larson LS, Uenishi GI, Hei D, Kelly K, Slukvin I, Rasko JEJ. Production, safety and efficacy of iPSC-derived mesenchymal stromal cells in acute steroid-resistant graft versus host disease: a phase I, multicenter, open-label, dose-escalation study. Nat Med. 2020;26:1720–5.
13. Yu J, Vodyanik MA, Smuga-Otto K, Antosiewicz-Bourget J, Frane JL, Tian S, Nie J, Jonsdottir GA, Ruotti V, Stewart R, Slukvin II, Thomson JA. Induced pluripotent stem cell lines derived from human somatic cells. Science. 2007;318:1917–20.
14. Cross J, Rai A, Fang H, Claridge B, Greening DW. Rapid and in-depth proteomic profiling of small extracellular vesicles for ultralow samples. Proteomics. 2024;24:e2300211.
15. Hughes CS, Moggridge S, Muller T, Sorensen PH, Morin GB, Krijgsveld J. Single-pot, solid-phase-enhanced sample Preparation for proteomics experiments. Nat Protoc. 2019;14:68–85.
16. Tham YK, Bernardo BC, Claridge B, Yildiz GS, Woon LM, Bond S, Fang H, Ooi JYY, Matsumoto A, Luo J, Tai CMK, Harmawan CA, Kiriazis H, Donner DG, Mellett NA, Abel ED, Khan SA, De Souza DP, Doomun SNE, Liu K, Xiang R, Singh M, Inouye M, Meikle PJ, Weeks KL, Drew BG, Greening DW, McMullen JR. Estrogen receptor alpha deficiency in cardiomyocytes reprograms the heart-derived extracellular vesicle proteome and induces obesity in female mice. Nat Cardiovasc Res. 2023;2:268–89.
17. Demichev V, Messner CB, Vernardis SI, Lilley KS, Ralser M. DIA-NN: neural networks and interference correction enable deep proteome coverage in high throughput. Nat Methods. 2020;17:41–4.
18. Fang H, Greening DW. An optimized Data-Independent acquisition strategy for comprehensive analysis of human plasma proteome. Methods Mol Biol. 2023;2628:93–107.
19. Ferdinandy P, Andreadou I, Baxter GF, Botker HE, Davidson SM, Dobrev D, Gersh BJ, Heusch G, Lecour S, Ruiz-Meana M, Zuurbier CJ, Hausenloy DJ, Schulz R. Interaction of cardiovascular nonmodifiable risk Factors, comorbidities and comedications with Ischemia/Reperfusion injury and cardioprotection by Pharmacological treatments and ischemic conditioning. Pharmacol Rev. 2023;75:159–216.
20. Behmenburg F, Heinen A, Bruch LV, Hollmann MW, Huhn R. Cardioprotection by remote ischemic preconditioning is blocked in the aged rat heart in vivo. J Cardiothorac Vasc Anesth. 2017;31:1223–6.
21. Boengler K, Buechert A, Heinen Y, Roeskes C, Hilfiker-Kleiner D, Heusch G, Schulz R. Cardioprotection by ischemic postconditioning is lost in aged and STAT3-deficient mice. Circ Res. 2008;102:131–5.
22. Wang Y, Yi H, Song Y. The safety of MSC therapy over the past 15 years: a meta-analysis. Stem Cell Res Ther. 2021;12:545.
23. Kavousi S, Hosseinpour A, Bahmanzadegan Jahromi F, Attar A. Efficacy of mesenchymal stem cell transplantation on major adverse cardiovascular events and cardiac function indices in patients with chronic heart failure: a meta-analysis of randomized controlled trials. J Transl Med. 2024;22:786.
24. Kelly K, Bloor AJC, Griffin JE, Radia R, Yeung DT, Rasko JEJ. Two-year safety outcomes of iPS cell-derived mesenchymal stromal cells in acute steroid-resistant graft-versus-host disease. Nat Med. 2024;30:1556–8.
25. Sharma A, Gupta S, Archana S, Verma RS. Emerging trends in mesenchymal stem cells applications for cardiac regenerative therapy: current status and advances. Stem Cell Rev Rep. 2022;18:1546–602.
26. Peng Y, Pan W, Ou Y, Xu W, Kaelber S, Borlongan CV, Sun M, Yu G. Extracardiac-Lodged mesenchymal stromal cells propel an inflammatory response against myocardial infarction via paracrine effects. Cell Transpl. 2016;25:929–35.
27. Deszcz I. Stem Cell-Based therapy and Cell-Free therapy as an alternative approach for cardiac regeneration. Stem Cells Int. 2023;2023:2729377.
28. Hwang HJ, Chang W, Song BW, Song H, Cha MJ, Kim IK, Lim S, Choi EJ, Ham O, Lee SY, Shim J, Joung B, Pak HN, Kim SS, Choi BR, Jang Y, Lee MH, Hwang KC. Antiarrhythmic potential of mesenchymal stem cell is modulated by hypoxic environment. J Am Coll Cardiol. 2012;60:1698–706.
29. Yeghiazarians Y, Zhang Y, Prasad M, Shih H, Saini SA, Takagawa J, Sievers RE, Wong ML, Kapasi NK, Mirsky R, Koskenvuo J, Minasi P, Ye J, Viswanathan MN, Angeli FS, Boyle AJ, Springer ML, Grossman W. Injection of bone marrow cell extract into infarcted hearts results in functional improvement comparable to intact cell therapy. Mol Ther. 2009;17:1250–6.
30. Alrefai MT, Tarola CL, Raagas R, Ridwan K, Shalal M, Lomis N, Paul A, Alrefai MD, Prakash S, Schwertani A, Shum-Tim D. Functional assessment of pluripotent and mesenchymal stem cell derived secretome in heart disease. Ann Stem Cell Res. 2019;2:29–36.
31. Angeli FS, Zhang Y, Sievers R, Jun K, Yim S, Boyle A, Yeghiazarians Y. Injection of human bone marrow and mononuclear cell extract into infarcted mouse hearts results in functional improvement. Open Cardiovasc Med J. 2012;6:38–43.
32. O'Neill HS, Gallagher LB, O'Sullivan J, Whyte W, Curley C, Dolan E, Hameed A, O'Dwyer J, Payne C, O'Reilly D, Ruiz-Hernandez E, Roche ET, O'Brien FJ, Cryan SA, Kelly H, Murphy B, Duffy GP. Biomaterial-Enhanced cell and drug delivery: lessons learned in the cardiac field and future perspectives. Adv Mater. 2016;28:5648–61.
33. Liguori TTA, Liguori GR, Sinkunas V, Correia CJ, Dos Santos Coutinho ESR, Zanoni FL, Aiello VD, Harmsen MC, Moreira LFP. Intrapericardial injection of hydrogels with ASC and their secretome to treat dilated cardiomyopathies. Sci Rep. 2025;15:3529.
34. Tang J, Wang J, Huang K, Ye Y, Su T, Qiao L, Hensley MT, Caranasos TG, Zhang J, Gu Z, Cheng K. Cardiac cell-integrated microneedle patch for treating myocardial infarction. Sci Adv. 2018;4:eaat9365.
35. Zhu D, Li Z, Huang K, Caranasos TG, Rossi JS, Cheng K. Minimally invasive delivery of therapeutic agents by hydrogel injection into the pericardial cavity for cardiac repair. Nat Commun. 2021;12:1412.
36. Preda MB, Ronningen T, Burlacu A, Simionescu M, Moskaug JO, Valen G. Remote transplantation of mesenchymal stem cells protects the heart against ischemia-reperfusion injury. Stem Cells. 2014;32:2123–34.
37. Liu Y, Yan S, Wu M, Xie Y, Sheng J, Sun X, Kang L, Xu B, Gu N. Subaxillary implantation of mesenchymal stem cell spheroids is a novel therapy for myocardial ischemia reperfusion injury. Chem Eng J. 2025;508.
38. Karbassi E, Yoo D, Martinson AM, Yang X, Reinecke H, Regnier M, Murry CE. Noncontractile stem Cell-Cardiomyocytes preserve Post-Infarction heart function. Circ Res. 2024;135:967–9.
39. Burt RK, Chen YH, Verda L, Lucena C, Navale S, Johnson J, Han X, Lomasney J, Baker JM, Ngai KL, Kino A, Carr J, Kajstura J, Anversa P. Mitotically inactivated embryonic stem cells can be used as an in vivo feeder layer to nurse damaged myocardium after acute myocardial infarction: a preclinical study. Circ Res. 2012;111:1286–96.
40. Vagnozzi RJ, Maillet M, Sargent MA, Khalil H, Johansen AKZ, Schwanekamp JA, York AJ, Huang V, Nahrendorf M, Sadayappan S, Molkentin JD. An acute immune response underlies the benefit of cardiac stem cell therapy. Nature. 2020;577:405–9.
41. Thum T, Bauersachs J, Poole-Wilson PA, Volk HD, Anker SD. The dying stem cell hypothesis: immune modulation as a novel mechanism for progenitor cell therapy in cardiac muscle. J Am Coll Cardiol. 2005;46:1799–802.
42. Preda MB, Neculachi CA, Fenyo IM, Vacaru AM, Publik MA, Simionescu M, Burlacu A. Short lifespan of syngeneic transplanted MSC is a consequence of in vivo apoptosis and immune cell recruitment in mice. Cell Death Dis. 2021;12:566.
43. Schmuck EG, Koch JM, Centanni JM, Hacker TA, Braun RK, Eldridge M, Hei DJ, Hematti P, Raval AN. Biodistribution and clearance of human mesenchymal stem cells by quantitative Three-Dimensional Cryo-Imaging after intravenous infusion in a rat lung injury model. Stem Cells Transl Med. 2016;5:1668–75.
44. van den Akker F, Feyen DA, van den Hoogen P, van Laake LW, van Eeuwijk EC, Hoefer I, Pasterkamp G, Chamuleau SA, Grundeman PF, Doevendans PA, Sluijter JP. Intramyocardial stem cell injection: go(ne) with the flow. Eur Heart J. 2017;38:184–6.
45. Mitchell AJ, Sabondjian E, Sykes J, Deans L, Zhu W, Lu X, Feng Q, Prato FS, Wisenberg G. Comparison of initial cell retention and clearance kinetics after subendocardial or subepicardial injections of endothelial progenitor cells in a canine myocardial infarction model. J Nucl Med. 2010;51:413–7.
46. Hodgson-Garms M, Moore MJ, Martino MM, Kelly K, Frith JE. Proteomic profiling of iPSC and tissue-derived MSC secretomes reveal a global signature of inflammatory licensing. NPJ Regen Med. 2025;10:7.
47. Romanazzo S, Kopecky C, Jiang S, Doshi R, Mukund V, Srivastava P, Rnjak-Kovacina J, Kelly K, Kilian KA. Biomaterials directed activation of a cryostable

therapeutic secretome in induced pluripotent stem cell derived mesenchymal stromal cells. J Tissue Eng Regen Med. 2022;16:1008–18.
48. Zhang Y, Zhang Z, Gao F, Tse HF, Tergaonkar V, Lian Q. Paracrine regulation in mesenchymal stem cells: the role of Rap1. Cell Death Dis. 2015;6:e1932.
49. Valencia J, Yanez RM, Muntion S, Fernandez-Garcia M, Martin-Rufino JD, Zapata AG, Bueren JA, Vicente A, Sanchez-Guijo F. Improving the therapeutic profile of mscs: cytokine priming reduces donor-dependent heterogeneity and enhances their Immunomodulatory capacity. Front Immunol. 2025;16:1473788.
50. Mack AA, Kroboth S, Rajesh D, Wang WB. Generation of induced pluripotent stem cells from CD34 + cells across blood drawn from multiple donors with non-integrating episomal vectors. PLoS ONE. 2011;6:e27956.

Publisher's Note

Springer Nature remains neutral with regard to jurisdictional claims in published maps and institutional affiliations.